## Characterization

Scanning electron microscope (SEM) images were obtained using a Hitachi HR-SEM SU8000 microscope at the accelerating voltage of 5.0 kV. Transmission electron microscope (TEM) and high-angle annular dark-field scanning TEM (HAADF-STEM) images were obtained using a JEOL JEM-2100F microscope at the accelerating voltage of 200 kV. The samples were prepared by drop casting the colloidal suspension on a carbon-coated copper grid. Low-angle X-ray diffraction (XRD) patterns were acquired by a Rigaku NANO-Viewer (Cu K$\alpha$) operated at 40 kV and 30 mA, while wide-angle XRD patterns were acquired by a Rigaku Rint 2500 diffractometer with monochromated Cu K$\alpha$ radiation. Cyclic voltammetry (CV) was carried out using a CHI 842B electrochemical analyzer. A conventional three-electrode cell was used, including an Ag/AgCl electrode as a reference electrode, a Pt wire as a counter electrode, and a glassy carbon electrode (GCE) modified by catalysts as a working electrode. Before the sample coating, the GCE was polished carefully with alumina powder and washed with deionized water, followed by drying with nitrogen gas. Then, the GCEs and the samples were dried completely at room temperature before the electrochemical experiments. The loading amounts of the samples were 5.0 μg.

**Fig. S1**

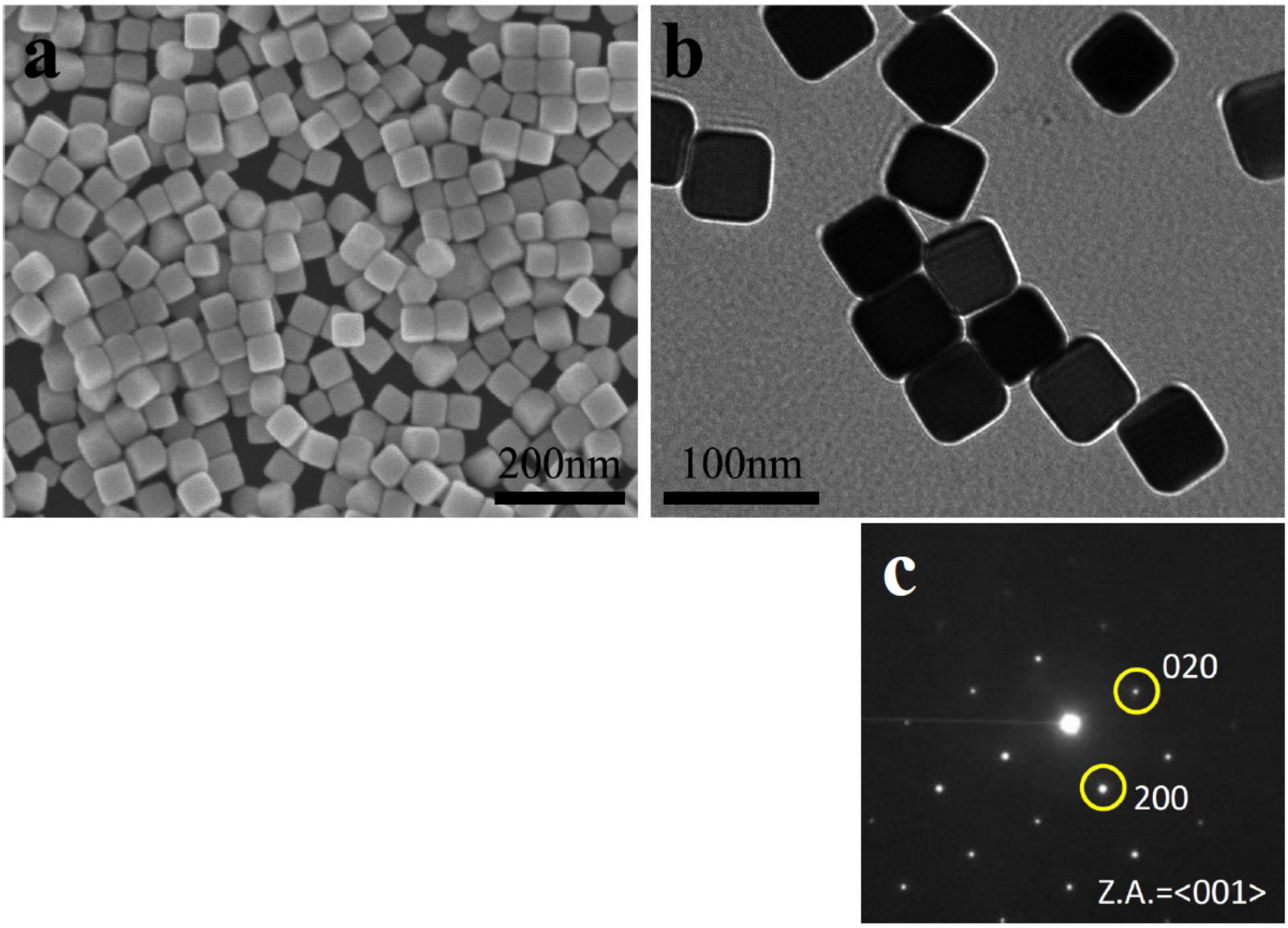

**Fig. S1** (a) SEM image and (b) TEM image Ag cubes synthesized by polyol process, and (c) selected-area ED patterns taken from one Ag cube in which the electron beam is applied perpendicular to the square face.

**Fig. S2**

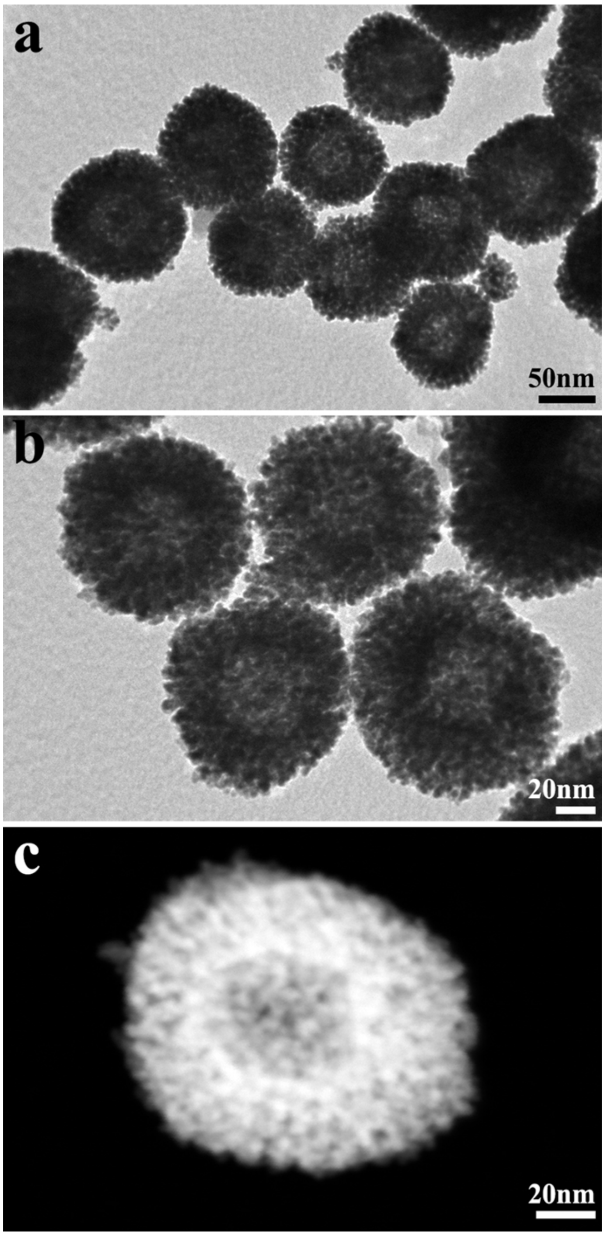

**Fig. S2** (a and b) Bright-field TEM images, and (c) HAADF-STEM image of MHPCs with thick shell prepared by using 6 µmol of $K_2PtCl_4$.

**Fig. S3**

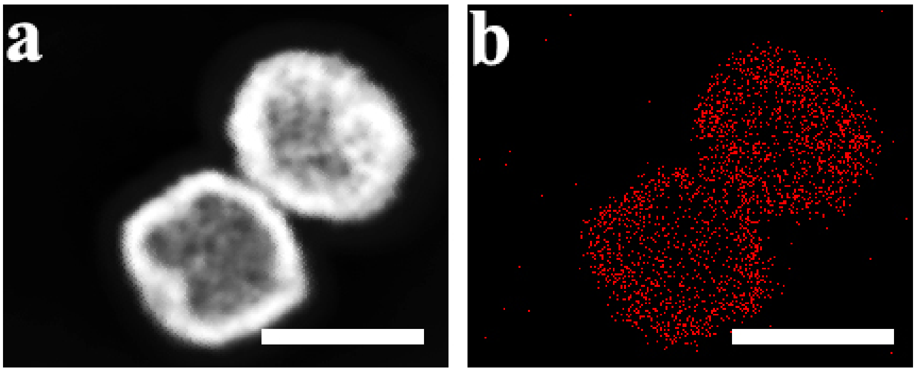

**Fig. S3** (a) HAADF-STEM image, and (b) Pt mapping of MHPCs after removal of Ag cores. The sample is prepared by using 1.6 μmol $K_2PtCl_4$. Scale bar is 50 nm.

**Fig. S4**

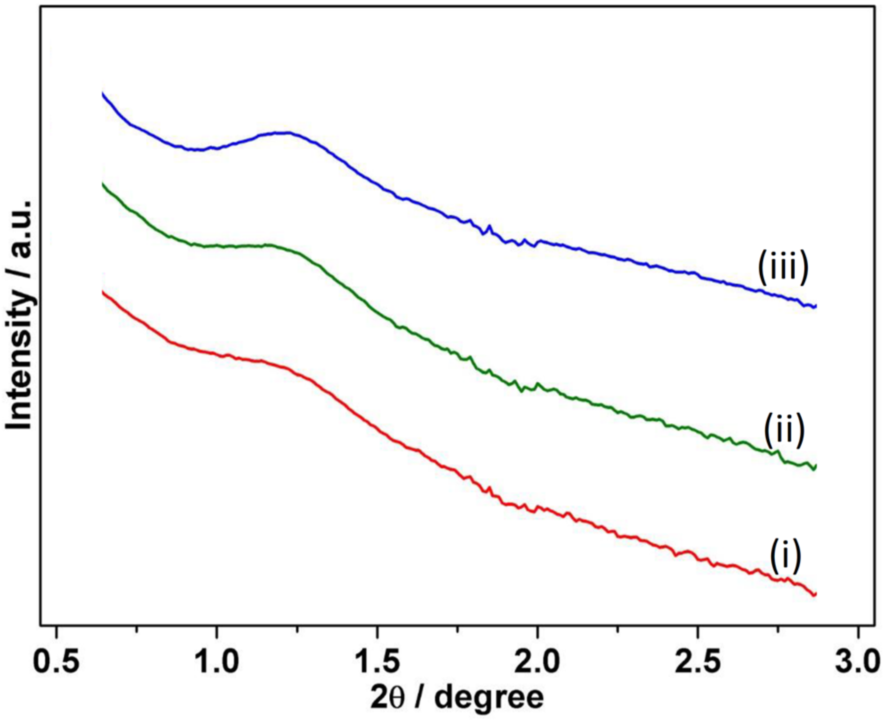

**Fig. S4** Low-angle XRD patterns of MHPCs with different shell thicknesses ((i) 5.0 nm, (ii) 5.5 nm, and (iii) 6.0 nm, respectively). With the increase of shell thicknesses, the peak intensities diffracted from the mesoporous structures are gradually increased.

**Fig. S5**

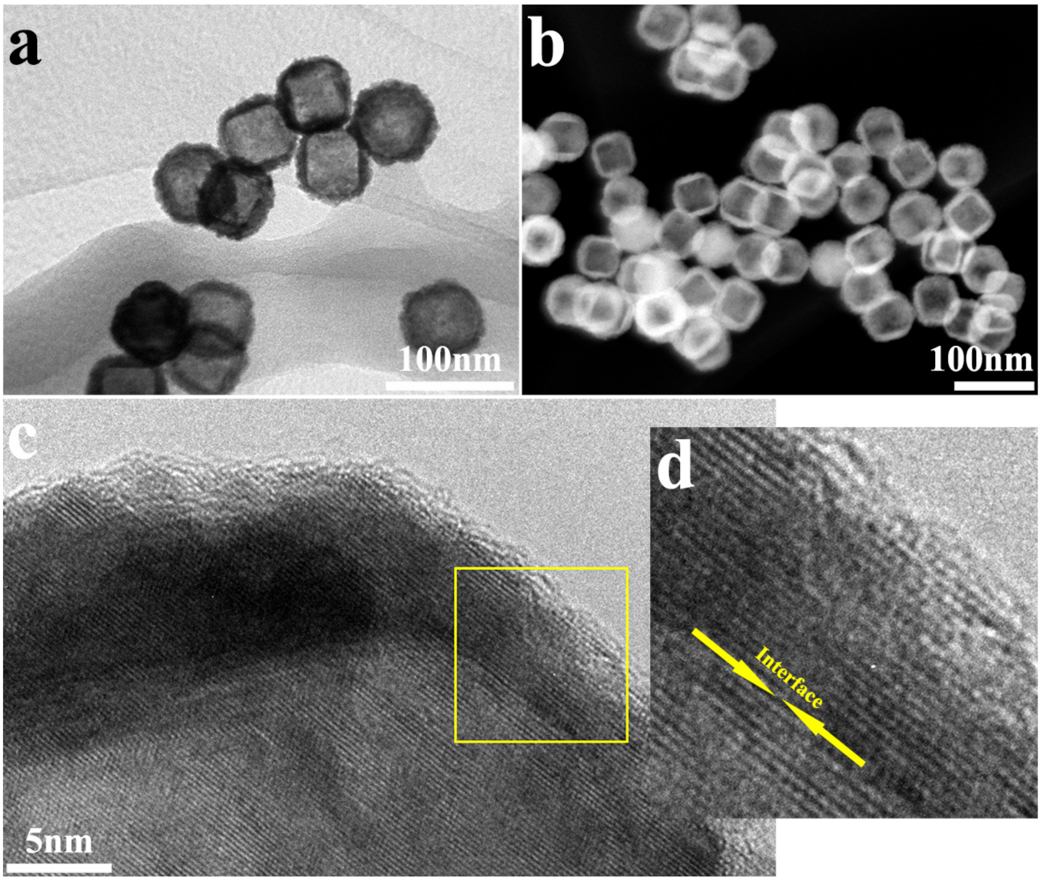

**Fig. S5** (a) Low-magnified bright-field TEM image, (b) HAADF-STEM image, and (c and d) HR-TEM images of hollow Pt cubes prepared without Brij58.

**Fig. S6**

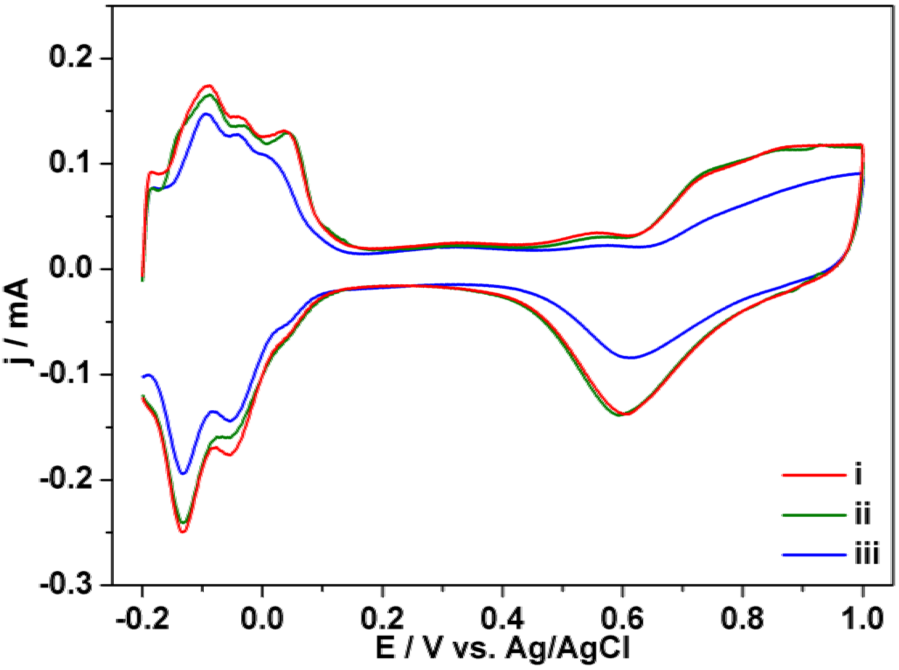

**Fig. S6** Cyclic voltammetric (CV) curves for the obtained MHPCs with various shell thicknesses recorded at room temperature in 0.5 M $H_2SO_4$ electrolyte at a sweep rate of 50 mV $s^{-1}$. The samples are prepared by using different amount of $K_2PtCl_4$ ((i) 0.8 μmol, (ii) 1.2 μmol, and (iii) 1.6 μmol, respectively). The electrochemical surface area (ECSA) is estimated by integrating the charge passed during the hydrogen adsorption/desorption region, assuming that the charge required to oxidize a mono-layer of hydrogen on bright Pt is 210 $\mu C \cdot cm^{-2}$.

**Fig. S7**

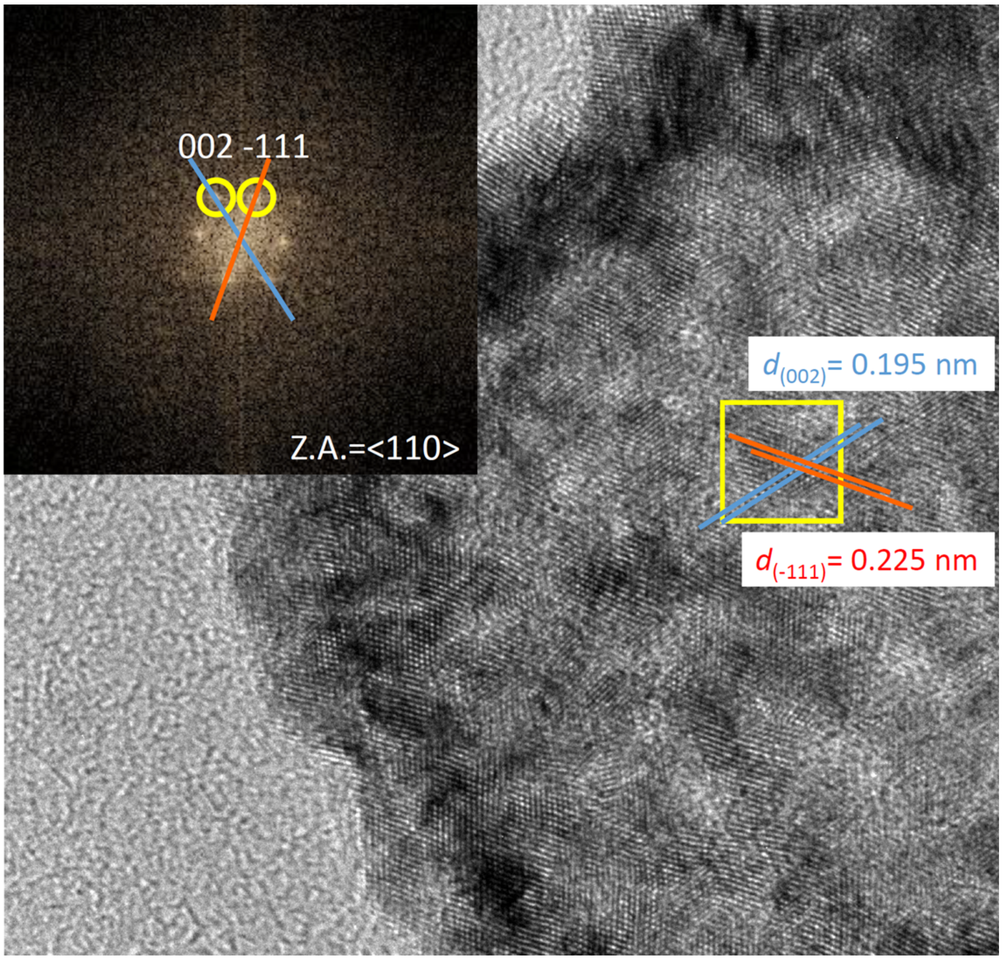

**Fig. S7** HR-TEM image of MHPCs with 5 nm shell thickness. The FFT image at the yellow square region is shown in the inset. Lattice fringes assignable to Pt *fcc* crystal are coherently extended through the whole part of MHPC.